



University of
Zurich^{UZH}

Zurich Open Repository and
Archive

University of Zurich
Main Library
Strickhofstrasse 39
CH-8057 Zurich
www.zora.uzh.ch

Year: 2013

W boson polarization measurement in the $t\bar{t}$ dilepton channel using the CDF II Detector

CDF Collaboration ; et al ; Canelli, F ; Kilminster, B

Abstract: We present a measurement of W boson polarization in top-quark decays in $t\bar{t}$ events with decays to dilepton final states using 5.1fb⁻¹ of integrated luminosity in $p\bar{p}$ collisions collected by the CDF II detector at the Tevatron. A simultaneous measurement of the fractions of longitudinal (f_0) and right-handed (f_+) W bosons yields the results $f_0=0.71+0.18-0.17(\text{stat})\pm 0.06(\text{syst})$ and $f_+=-0.07\pm 0.09(\text{stat})\pm 0.03(\text{syst})$. Combining this measurement with our previous result based on single lepton final states, we obtain $f_0=0.84\pm 0.09(\text{stat})\pm 0.05(\text{syst})$ and $f_+=-0.16\pm 0.05(\text{stat})\pm 0.04(\text{syst})$. The results are consistent with standard model expectation.

DOI: <https://doi.org/10.1016/j.physletb.2013.03.032>

Posted at the Zurich Open Repository and Archive, University of Zurich

ZORA URL: <https://doi.org/10.5167/uzh-92117>

Journal Article

Accepted Version

Originally published at:

CDF Collaboration; et al; Canelli, F; Kilminster, B (2013). W boson polarization measurement in the $t\bar{t}$ dilepton channel using the CDF II Detector. *Physics Letters B*, 722(1-3):48-54.

DOI: <https://doi.org/10.1016/j.physletb.2013.03.032>

W-boson polarization measurement in the $t\bar{t}$ dilepton channel using the CDF II Detector

T. Aaltonen,²¹ B. Álvarez González^{z,9} S. Amerio,⁴⁰ D. Amidei,³² A. Anastassov^{x,15} A. Annovi,¹⁷ J. Antos,¹² G. Apollinari,¹⁵ J.A. Appel,¹⁵ T. Arisawa,⁵⁴ A. Artikov,¹³ J. Asaadi,⁴⁹ W. Ashmanskas,¹⁵ B. Auerbach,⁵⁷ A. Aurisano,⁴⁹ F. Azfar,³⁹ W. Badgett,¹⁵ T. Bae,²⁵ A. Barbaro-Galtieri,²⁶ V.E. Barnes,⁴⁴ B.A. Barnett,²³ P. Barria^{hh,42} P. Bartos,¹² M. Bauce^{ff,40} F. Bedeschi,⁴² S. Behari,²³ G. Bellettini^{gg,42} J. Bellinger,⁵⁶ D. Benjamin,¹⁴ A. Beretvas,¹⁵ A. Bhatti,⁴⁶ D. Bisello^{ff,40} I. Bizjak,²⁸ K.R. Bland,⁵ B. Blumenfeld,²³ A. Bocci,¹⁴ A. Bodek,⁴⁵ D. Bortoletto,⁴⁴ J. Boudreau,⁴³ A. Boveia,¹¹ L. Brigliadori^{ee,6} C. Bromberg,³³ E. Brucken,²¹ J. Budagov,¹³ H.S. Budd,⁴⁵ K. Burkett,¹⁵ G. Busetto^{ff,40} P. Bussey,¹⁹ A. Buzatu,³¹ A. Calamba,¹⁰ C. Calancha,²⁹ S. Camarda,⁴ M. Campanelli,²⁸ M. Campbell,³² F. Canelli,^{11,15} B. Carls,²² D. Carlsmith,⁵⁶ R. Carosi,⁴² S. Carrillo^{m,16} S. Carron,¹⁵ B. Casal^{k,9} M. Casarsa,⁵⁰ A. Castro^{ee,6} P. Catastini,²⁰ D. Cauz,⁵⁰ V. Cavaliere,²² M. Cavalli-Sforza,⁴ A. Cerri^{f,26} L. Cerrito^{s,28} Y.C. Chen,¹ M. Chertok,⁷ G. Chiarelli,⁴² G. Chlachidze,¹⁵ F. Chlebana,¹⁵ K. Cho,²⁵ D. Chokheli,¹³ W.H. Chung,⁵⁶ Y.S. Chung,⁴⁵ M.A. Ciocci^{hh,42} A. Clark,¹⁸ C. Clarke,⁵⁵ G. Compostella^{ff,40} M.E. Convery,¹⁵ J. Conway,⁷ M. Corbo,¹⁵ M. Cordelli,¹⁷ C.A. Cox,⁷ D.J. Cox,⁷ F. Crescioli^{gg,42} J. Cuevas^{z,9} R. Culbertson,¹⁵ D. Dagenhart,¹⁵ N. d'Ascenzo^{w,15} M. Datta,¹⁵ P. de Barbaro,⁴⁵ M. Dell'Orso^{gg,42} L. Demortier,⁴⁶ M. Deninno,⁶ F. Devoto,²¹ M. d'Errico^{ff,40} A. Di Canto^{gg,42} B. Di Ruzza,¹⁵ J.R. Dittmann,⁵ M. D'Onofrio,²⁷ S. Donati^{gg,42} P. Dong,¹⁵ M. Dorigo,⁵⁰ T. Dorigo,⁴⁰ K. Ebina,⁵⁴ A. Elagin,⁴⁹ A. Eppig,³² R. Erbacher,⁷ S. Errede,²² N. Ershaidat^{dd,15} R. Eusebi,⁴⁹ S. Farrington,³⁹ M. Feindt,²⁴ J.P. Fernandez,²⁹ R. Field,¹⁶ G. Flanagan^{u,15} R. Forrest,⁷ M.J. Frank,⁵ M. Franklin,²⁰ J.C. Freeman,¹⁵ Y. Funakoshi,⁵⁴ I. Furic,¹⁶ M. Gallinaro,⁴⁶ J.E. Garcia,¹⁸ A.F. Garfinkel,⁴⁴ P. Garosi^{hh,42} H. Gerberich,²² E. Gerchtein,¹⁵ S. Giagu,⁴⁷ V. Giakoumopoulou,³ P. Giannetti,⁴² K. Gibson,⁴³ C.M. Ginsburg,¹⁵ N. Giokaris,³ P. Giromini,¹⁷ G. Giurgiu,²³ V. Glagolev,¹³ D. Glenzinski,¹⁵ M. Gold,³⁵ D. Goldin,⁴⁹ N. Goldschmidt,¹⁶ A. Golossanov,¹⁵ G. Gomez,⁹ G. Gomez-Ceballos,³⁰ M. Goncharov,³⁰ O. González,²⁹ I. Gorelov,³⁵ A.T. Goshaw,¹⁴ K. Goulianos,⁴⁶ S. Grinstein,⁴ C. Grosso-Pilcher,¹¹ R.C. Group^{53,15} J. Guimaraes da Costa,²⁰ S.R. Hahn,¹⁵ E. Halkiadakis,⁴⁸ A. Hamaguchi,³⁸ J.Y. Han,⁴⁵ F. Happacher,¹⁷ K. Hara,⁵¹ D. Hare,⁴⁸ M. Hare,⁵² R.F. Harr,⁵⁵ K. Hatakeyama,⁵ C. Hays,³⁹ M. Heck,²⁴ J. Heinrich,⁴¹ M. Herndon,⁵⁶ S. Hewamanage,⁵ A. Hocker,¹⁵ W. Hopkins^{g,15} D. Horn,²⁴ S. Hou,¹ R.E. Hughes,³⁶ M. Hurwitz,¹¹ U. Husemann,⁵⁷ N. Hussain,³¹ M. Hussein,³³ J. Huston,³³ G. Introzzi,⁴² M. Iori^{jj,47} A. Ivanov^{p,7} E. James,¹⁵ D. Jang,¹⁰ B. Jayatilaka,¹⁴ E.J. Jeon,²⁵ S. Jindariani,¹⁵ M. Jones,⁴⁴ K.K. Joo,²⁵ S.Y. Jun,¹⁰ T.R. Junk,¹⁵ T. Kamon^{25,49} P.E. Karchin,⁵⁵ A. Kashi,⁵ Y. Kato^{o,38} W. Ketchum,¹¹ J. Keung,⁴¹ V. Khotilovich,⁴⁹ B. Kilminster,¹⁵ D.H. Kim,²⁵ H.S. Kim,²⁵ J.E. Kim,²⁵ M.J. Kim,¹⁷ S.B. Kim,²⁵ S.H. Kim,⁵¹ Y.K. Kim,¹¹ Y.J. Kim,²⁵ N. Kimura,⁵⁴ M. Kirby,¹⁵ S. Klimenko,¹⁶ K. Knoepfel,¹⁵ K. Kondo^{*,54} D.J. Kong,²⁵ J. Konigsberg,¹⁶ A.V. Kotwal,¹⁴ M. Kreps,²⁴ J. Kroll,⁴¹ D. Krop,¹¹ M. Kruse,¹⁴ V. Krutelyov^{c,49} T. Kuhr,²⁴ M. Kurata,⁵¹ S. Kwang,¹¹ A.T. Laasanen,⁴⁴ S. Lami,⁴² S. Lammel,¹⁵ M. Lancaster,²⁸ R.L. Lander,⁷ K. Lannon^{y,36} A. Lath,⁴⁸ G. Latino^{hh,42} T. LeCompte,² E. Lee,⁴⁹ H.S. Lee^{q,11} J.S. Lee,²⁵ S.W. Lee^{bb,49} S. Leo^{gg,42} S. Leone,⁴² J.D. Lewis,¹⁵ A. Limosani^{t,14} C.-J. Lin,²⁶ M. Lindgren,¹⁵ E. Lipeles,⁴¹ A. Lister,¹⁸ D.O. Litvintsev,¹⁵ C. Liu,⁴³ H. Liu,⁵³ Q. Liu,⁴⁴ T. Liu,¹⁵ S. Lockwitz,⁵⁷ A. Loginov,⁵⁷ D. Lucchesi^{ff,40} J. Lueck,²⁴ P. Lujan,²⁶ P. Lukens,¹⁵ G. Lungu,⁴⁶ J. Lys,²⁶ R. Lysak^{e,12} R. Madrak,¹⁵ K. Maeshima,¹⁵ P. Maestro^{hh,42} S. Malik,⁴⁶ G. Manca^{a,27} A. Manousakis-Katsikakis,³ F. Margaroli,⁴⁷ C. Marino,²⁴ M. Martínez,⁴ P. Mastrandrea,⁴⁷ K. Matera,²² M.E. Mattson,⁵⁵ A. Mazzacane,¹⁵ P. Mazzanti,⁶ K.S. McFarland,⁴⁵ P. McIntyre,⁴⁹ R. McNulty^{j,27} A. Mehta,²⁷ P. Mehtala,²¹ C. Mesropian,⁴⁶ T. Miao,¹⁵ D. Mietlicki,³² A. Mitra,¹ H. Miyake,⁵¹ S. Moed,¹⁵ N. Moggi,⁶ M.N. Mondragon^{m,15} C.S. Moon,²⁵ R. Moore,¹⁵ M.J. Morello^{ii,42} J. Morlock,²⁴ P. Movilla Fernandez,¹⁵ A. Mukherjee,¹⁵ Th. Muller,²⁴ P. Murat,¹⁵ M. Mussini^{ee,6} J. Nachtman^{n,15} Y. Nagai,⁵¹ J. Naganoma,⁵⁴ I. Nakano,³⁷ A. Napier,⁵² J. Nett,⁴⁹ C. Neu,⁵³ M.S. Neubauer,²² J. Nielsen^{d,26} L. Nodulman,² S.Y. Noh,²⁵ O. Norriella,²² L. Oakes,³⁹ S.H. Oh,¹⁴ Y.D. Oh,²⁵ I. Oksuzian,⁵³ T. Okusawa,³⁸ R. Orava,²¹ L. Ortolan,⁴ S. Pagan Griso^{ff,40} C. Pagliarone,⁵⁰ E. Palencia^{f,9} V. Papadimitriou,¹⁵ A.A. Paramonov,² J. Patrick,¹⁵ G. Pauletta^{kk,50} M. Paulini,¹⁰ C. Paus,³⁰ D.E. Pellett,⁷ A. Penzo,⁵⁰ T.J. Phillips,¹⁴ G. Piacentino,⁴² E. Pianori,⁴¹ J. Pilot,³⁶ K. Pitts,²² C. Plager,⁸ L. Pondrom,⁵⁶ S. Poprocki^{g,15} K. Potamianos,⁴⁴ F. Prokoshin^{cc,13} A. Pranko,²⁶ F. Ptohos^{h,17} G. Punzi^{gg,42} A. Rahaman,⁴³ V. Ramakrishnan,⁵⁶ N. Ranjan,⁴⁴ I. Redondo,²⁹ P. Renton,³⁹ M. Rescigno,⁴⁷ T. Riddick,²⁸ F. Rimondi^{ee,6} L. Ristori^{42,15} A. Robson,¹⁹ T. Rodrigo,⁹ T. Rodriguez,⁴¹ E. Rogers,²² S. Rolli^{i,52} R. Roser,¹⁵ F. Ruffini^{hh,42} A. Ruiz,⁹ J. Russ,¹⁰ V. Rusu,¹⁵ A. Safonov,⁴⁹ W.K. Sakumoto,⁴⁵ Y. Sakurai,⁵⁴ L. Santi^{kk,50} K. Sato,⁵¹

V. Saveliev^{w,15} A. Savoy-Navarro^{aa,15} P. Schlabach,¹⁵ A. Schmidt,²⁴ E.E. Schmidt,¹⁵ T. Schwarz,¹⁵ L. Scodellaro,⁹ A. Scribano^{hh,42} F. Scuri,⁴² S. Seidel,³⁵ Y. Seiya,³⁸ A. Semenov,¹³ F. Sforza^{hh,42} S.Z. Shalhout,⁷ T. Shears,²⁷ P.F. Shepard,⁴³ M. Shimojima^{v,51} M. Shochet,¹¹ I. Shreyber-Tecker,³⁴ A. Simonenko,¹³ P. Sinervo,³¹ K. Sliwa,⁵² J.R. Smith,⁷ F.D. Snider,¹⁵ A. Soha,¹⁵ V. Sorin,⁴ H. Song,⁴³ P. Squillacioti^{hh,42} M. Stancari,¹⁵ R. St. Denis,¹⁹ B. Stelzer,³¹ O. Stelzer-Chilton,³¹ D. Stentz^{x,15} J. Strologas,³⁵ G.L. Strycker,³² Y. Sudo,⁵¹ A. Sukhanov,¹⁵ I. Suslov,¹³ K. Takemasa,⁵¹ Y. Takeuchi,⁵¹ J. Tang,¹¹ M. Tecchio,³² P.K. Teng,¹ J. Thom^{g,15} J. Thome,¹⁰ G.A. Thompson,²² E. Thomson,⁴¹ D. Toback,⁴⁹ S. Tokar,¹² K. Tollefson,³³ T. Tomura,⁵¹ D. Tonelli,¹⁵ S. Torre,¹⁷ D. Torretta,¹⁵ P. Totaro,⁴⁰ M. Trovato^{ii,42} F. Ukegawa,⁵¹ S. Uozumi,²⁵ A. Varganov,³² F. Vázquez^{m,16} G. Velev,¹⁵ C. Vellidis,¹⁵ M. Vidal,⁴⁴ I. Vila,⁹ R. Vilar,⁹ J. Vizán,⁹ M. Vogel,³⁵ G. Volpi,¹⁷ P. Wagner,⁴¹ R.L. Wagner,¹⁵ T. Wakisaka,³⁸ R. Wallny,⁸ S.M. Wang,¹ A. Warburton,³¹ D. Waters,²⁸ W.C. Wester III,¹⁵ D. Whiteson^{b,41} A.B. Wicklund,² E. Wicklund,¹⁵ S. Wilbur,¹¹ F. Wick,²⁴ H.H. Williams,⁴¹ J.S. Wilson,³⁶ P. Wilson,¹⁵ B.L. Winer,³⁶ P. Wittich^{g,15} S. Wolbers,¹⁵ H. Wolfe,³⁶ T. Wright,³² X. Wu,¹⁸ Z. Wu,⁵ K. Yamamoto,³⁸ D. Yamato,³⁸ T. Yang,¹⁵ U.K. Yang^{r,11} Y.C. Yang,²⁵ W.-M. Yao,²⁶ G.P. Yeh,¹⁵ K. Yi^{n,15} J. Yoh,¹⁵ K. Yorita,⁵⁴ T. Yoshida^{l,38} G.B. Yu,¹⁴ I. Yu,²⁵ S.S. Yu,¹⁵ J.C. Yun,¹⁵ A. Zanetti,⁵⁰ Y. Zeng,¹⁴ C. Zhou,¹⁴ and S. Zucchelli^{ee6}
(CDF Collaboration[†])

The CDF collaboration

¹*Institute of Physics, Academia Sinica, Taipei, Taiwan 11529, Republic of China*

²*Argonne National Laboratory, Argonne, Illinois 60439, USA*

³*University of Athens, 157 71 Athens, Greece*

⁴*Institut de Física d'Altes Energies, ICREA, Universitat Autònoma de Barcelona, E-08193, Bellaterra (Barcelona), Spain*

⁵*Baylor University, Waco, Texas 76798, USA*

⁶*Istituto Nazionale di Fisica Nucleare Bologna, ^{ee}University of Bologna, I-40127 Bologna, Italy*

⁷*University of California, Davis, Davis, California 95616, USA*

⁸*University of California, Los Angeles, Los Angeles, California 90024, USA*

⁹*Instituto de Física de Cantabria, CSIC-University of Cantabria, 39005 Santander, Spain*

¹⁰*Carnegie Mellon University, Pittsburgh, Pennsylvania 15213, USA*

¹¹*Enrico Fermi Institute, University of Chicago, Chicago, Illinois 60637, USA*

¹²*Comenius University, 842 48 Bratislava, Slovakia; Institute of Experimental Physics, 040 01 Kosice, Slovakia*

¹³*Joint Institute for Nuclear Research, RU-141980 Dubna, Russia*

¹⁴*Duke University, Durham, North Carolina 27708, USA*

¹⁵*Fermi National Accelerator Laboratory, Batavia, Illinois 60510, USA*

¹⁶*University of Florida, Gainesville, Florida 32611, USA*

¹⁷*Laboratori Nazionali di Frascati, Istituto Nazionale di Fisica Nucleare, I-00044 Frascati, Italy*

¹⁸*University of Geneva, CH-1211 Geneva 4, Switzerland*

¹⁹*Glasgow University, Glasgow G12 8QQ, United Kingdom*

²⁰*Harvard University, Cambridge, Massachusetts 02138, USA*

²¹*Division of High Energy Physics, Department of Physics,*

University of Helsinki and Helsinki Institute of Physics, FIN-00014, Helsinki, Finland

²²*University of Illinois, Urbana, Illinois 61801, USA*

²³*The Johns Hopkins University, Baltimore, Maryland 21218, USA*

²⁴*Institut für Experimentelle Kernphysik, Karlsruhe Institute of Technology, D-76131 Karlsruhe, Germany*

²⁵*Center for High Energy Physics: Kyungpook National University,*

Daegu 702-701, Korea; Seoul National University, Seoul 151-742,

Korea; Sungkyunkwan University, Suwon 440-746,

Korea; Korea Institute of Science and Technology Information,

Daejeon 305-806, Korea; Chonnam National University, Gwangju 500-757,

Korea; Chonbuk National University, Jeonju 561-756, Korea

²⁶*Ernest Orlando Lawrence Berkeley National Laboratory, Berkeley, California 94720, USA*

²⁷*University of Liverpool, Liverpool L69 7ZE, United Kingdom*

²⁸*University College London, London WC1E 6BT, United Kingdom*

²⁹*Centro de Investigaciones Energeticas Medioambientales y Tecnológicas, E-28040 Madrid, Spain*

³⁰*Massachusetts Institute of Technology, Cambridge, Massachusetts 02139, USA*

³¹*Institute of Particle Physics: McGill University, Montréal, Québec,*

Canada H3A 2T8; Simon Fraser University, Burnaby, British Columbia,

Canada V5A 1S6; University of Toronto, Toronto, Ontario,

Canada M5S 1A7; and TRIUMF, Vancouver, British Columbia, Canada V6T 2A3

³²*University of Michigan, Ann Arbor, Michigan 48109, USA*

³³*Michigan State University, East Lansing, Michigan 48824, USA*

³⁴*Institution for Theoretical and Experimental Physics, ITEP, Moscow 117259, Russia*

³⁵*University of New Mexico, Albuquerque, New Mexico 87131, USA*

³⁶*The Ohio State University, Columbus, Ohio 43210, USA*

³⁷*Okayama University, Okayama 700-8530, Japan*

³⁸*Osaka City University, Osaka 588, Japan*

³⁹*University of Oxford, Oxford OX1 3RH, United Kingdom*

⁴⁰*Istituto Nazionale di Fisica Nucleare, Sezione di Padova-Trento, ^{ff}University of Padova, I-35131 Padova, Italy*

⁴¹*University of Pennsylvania, Philadelphia, Pennsylvania 19104, USA*

⁴²*Istituto Nazionale di Fisica Nucleare Pisa, ^{gg}University of Pisa,*

^{hh}*University of Siena and ⁱⁱScuola Normale Superiore, I-56127 Pisa, Italy*

⁴³*University of Pittsburgh, Pittsburgh, Pennsylvania 15260, USA*

⁴⁴*Purdue University, West Lafayette, Indiana 47907, USA*

⁴⁵*University of Rochester, Rochester, New York 14627, USA*

⁴⁶*The Rockefeller University, New York, New York 10065, USA*

⁴⁷*Istituto Nazionale di Fisica Nucleare, Sezione di Roma 1,*

^{jj}*Sapienza Università di Roma, I-00185 Roma, Italy*

⁴⁸*Rutgers University, Piscataway, New Jersey 08855, USA*

⁴⁹*Texas A&M University, College Station, Texas 77843, USA*

⁵⁰*Istituto Nazionale di Fisica Nucleare Trieste/Udine, I-34100 Trieste, ^{kk}University of Udine, I-33100 Udine, Italy*

⁵¹*University of Tsukuba, Tsukuba, Ibaraki 305, Japan*

⁵²*Tufts University, Medford, Massachusetts 02155, USA*

⁵³*University of Virginia, Charlottesville, Virginia 22906, USA*

⁵⁴*Waseda University, Tokyo 169, Japan*

⁵⁵*Wayne State University, Detroit, Michigan 48201, USA*

⁵⁶*University of Wisconsin, Madison, Wisconsin 53706, USA*

⁵⁷*Yale University, New Haven, Connecticut 06520, USA*

(Dated: September 18, 2013)

We present a measurement of the W -boson polarization in top-quark decays in $t\bar{t}$ events with decays to dilepton final states using data corresponding to 5.1 fb^{-1} of integrated luminosity in $p\bar{p}$ collisions collected by the CDF II detector at the Tevatron. Assuming a top-quark mass of $172.5 \text{ GeV}/c^2$, a simultaneous measurement of the fractions of longitudinal (f_0) and right-handed (f_+) W -bosons yields the results $f_0 = 0.70_{-0.17}^{+0.18}(\text{stat}) \pm 0.06(\text{syst})$ and $f_+ = -0.09 \pm 0.09(\text{stat}) \pm 0.03(\text{syst})$. Combining this measurement with our previous measurement based on single-lepton final states, we obtain $f_0 = 0.84 \pm 0.09(\text{stat}) \pm 0.05(\text{syst})$ and $f_+ = -0.16 \pm 0.05(\text{stat}) \pm 0.04(\text{syst})$. The results are consistent with the standard model expectation.

PACS numbers: 14.65.Ha, 12.15.Ji, 13.38.Be, 13.88.+e

*Deceased

†With visitors from ^aIstituto Nazionale di Fisica Nucleare, Sezione di Cagliari, 09042 Monserrato (Cagliari), Italy, ^bUniversity of CA Irvine, Irvine, CA 92697, USA, ^cUniversity of CA Santa Barbara, Santa Barbara, CA 93106, USA, ^dUniversity of CA Santa Cruz, Santa Cruz, CA 95064, USA, ^eInstitute of Physics, Academy of Sciences of the Czech Republic, Czech Republic, ^fCERN, CH-1211 Geneva, Switzerland, ^gCornell University, Ithaca, NY 14853, USA, ^hUniversity of Cyprus, Nicosia CY-1678, Cyprus, ⁱOffice of Science, U.S. Department of Energy, Washington, DC 20585, USA, ^jUniversity College Dublin, Dublin 4, Ireland, ^kETH, 8092 Zurich, Switzerland, ^lUniversity of Fukui, Fukui City, Fukui Prefecture, Japan 910-0017, ^mUniversidad Iberoamericana, Mexico D.F., Mexico, ⁿUniversity of Iowa, Iowa City, IA 52242, USA, ^oKinki University, Higashi-Osaka City, Japan 577-8502, ^pKansas State University, Manhattan, KS 66506, USA, ^qKorea University, Seoul, 136-713, Korea, ^rUniversity of Manchester, Manchester M13 9PL, United Kingdom, ^sQueen Mary, University of London, London, E1 4NS, United Kingdom, ^tUniversity of Melbourne, Victoria 3010, Australia, ^uMuons, Inc., Batavia, IL 60510, USA, ^vNagasaki Institute of Applied Science, Nagasaki, Japan, ^wNational Research Nuclear University, Moscow, Russia, ^xNorthwestern University,

Since the top quark discovery by the CDF and D0 experiments in 1995, many of its properties have been measured. Due to its very short lifetime [1, 2], the top quark does not hadronize and therefore its properties are transferred directly to its decay products. The standard model (SM) makes specific predictions for the W -boson polarization in top-quark decays. Precise measurement of the W -boson polarization provides a test of the SM and could reveal new physics beyond the SM [3].

In the SM, the top quark decays to a W -boson and b quark with almost 100% probability [4]. The W -boson is a massive vector particle with three polariza-

Evanston, IL 60208, USA, ^yUniversity of Notre Dame, Notre Dame, IN 46556, USA, ^zUniversidad de Oviedo, E-33007 Oviedo, Spain, ^{aa}CNRS-IN2P3, Paris, F-75205 France, ^{bb}Texas Tech University, Lubbock, TX 79609, USA, ^{cc}Universidad Tecnica Federico Santa Maria, 110v Valparaiso, Chile, ^{dd}Yarmouk University, Irbid 211-63, Jordan,

tion states: right-handed (+1), longitudinal (0), and left-handed (-1). The differential decay rate of the top quark is given by:

$$\frac{d\Gamma}{d\cos\theta^*} \propto (1 - \cos\theta^*)^2 f_- + 2(1 - \cos^2\theta^*) f_0 + (1 + \cos\theta^*)^2 f_+ \quad (1)$$

where θ^* is the angle between the direction of the charged lepton (or down-type quark from the decay of the W -boson) and the opposite direction of the top quark in the W -boson rest frame. The polarization fractions satisfy the normalization condition $f_- + f_0 + f_+ = 1$. The right-handed W -boson production in the context of the SM is strongly suppressed due to the $V - A$ structure of the charged-current weak interaction. In the SM at the tree level [3], the fraction of right-handed W -bosons is very close to zero ($f_+ = 3.7 \times 10^{-4}$) while $f_0 = 0.698$ and $f_- = 0.301$ for a top-quark mass (m_{top}) of 173.3 GeV/ c^2 [5], a W -boson mass (m_W) of 80.4 GeV/ c^2 [4], and a b -quark mass (m_b) of 4.78 GeV/ c^2 [4]. In the $m_b \rightarrow 0$ limit, $f_+ = 0$ and $f_0 = m_{top}^2 / (2m_W^2 + m_{top}^2)$. Polarization fractions that deviate from the SM values are predicted in theories with anomalous tWb couplings [3].

An earlier measurement of the polarization fractions of the W -boson in top-quark decays by the CDF collaboration focused on the single-lepton channel [6]. Results have also been reported by the D0 and ATLAS collaborations, where the measurements in the single-lepton and dilepton channels are combined [7, 8]. In this Letter we report the CDF measurement in the dilepton channel ($t\bar{t} \rightarrow W^+bW^- \bar{b} \rightarrow \ell^+\nu b\ell^-\bar{\nu}\bar{b}$) where $\ell = e, \mu$ and leptonically decaying τ leptons are also included into the signal. We perform two types of measurements: a model-independent approach where f_0 and f_+ are determined simultaneously; and a model-dependent approach where f_0 (f_+) is fixed to its SM value, and f_+ (f_0) is measured. The model-independent and model-dependent approaches are referred as “2D” and “1D”, respectively, throughout this article. We also combine this result with our previous measurement [6] in the single-lepton channel.

This analysis is based on data corresponding to an integrated luminosity of 5.1 fb $^{-1}$ collected with the CDF II detector [9] between March 2002 and June 2009 at the Fermilab Tevatron with a center of mass energy $\sqrt{s} = 1.96$ TeV. The CDF II detector is described in detail elsewhere [9]. The components essential to this analysis are the tracking system consisting of a silicon microstrip tracker and a central drift chamber immersed in a 1.4 T solenoidal magnetic field, electromagnetic and hadronic calorimeters arranged in a projective geometry outside the magnet coil, and drift chambers and scintillation counters for muon detection outside the calorimeters.

The analysis uses the same event selection criteria that were used for the measurement of the $t\bar{t}$ cross-section in the dilepton channel [10]. A brief description of the event selection is as follows: the data were collected

with an online inclusive event-selection system (trigger) that requires a lepton (electron or muon) with transverse energy $E_T > 18$ GeV. From the inclusive lepton data, we select events with oppositely-charged leptons of $E_T > 20$ GeV. We define leptons to satisfy very restrictive identification and isolation criteria as “tight” while “loose” leptons satisfy less restrictive identification criteria and has no isolation requirement. We require at least one tight lepton in each dilepton candidate. The pseudorapidity η [11] coverage is $|\eta| < 2.0$ for electrons and $|\eta| < 1.0$ for muons. We require missing transverse energy $\cancel{E}_T > 25$ GeV [13] unless the \cancel{E}_T direction is along (within 20° in ϕ) either a lepton or a jet, in which case we require $\cancel{E}_T > 50$ GeV. Additionally we require at least two jets [14] reconstructed with $E_T > 15$ GeV and $|\eta| < 2.5$. Jet energies are corrected for the effects of calorimeter response, multiple interactions, and the hadronic calorimeter energy scale [15]. Background contributions are further reduced through kinematic cuts on the dilepton invariant mass, total energy in the transverse plane and \cancel{E}_T significance [10]. In this measurement, we split the inclusive data sample into two non-overlapping subsamples (“ b -tag” and “non-tag”) where for the “ b -tag” subsample we require at least one jet in the event to be consistent with having originated from a b quark by using an algorithm that identifies a long-lived b hadron through the presence of a displaced vertex [16]. The two subsamples have different signal-to-background ratios and background compositions; therefore, we can improve the overall measurement uncertainties by analyzing each subsample separately.

The dominant background contribution is from “fake” events where a jet is misidentified as a lepton. The main source of “fake” events is $W(\rightarrow \ell\nu) + \text{jets}$ events. An additional background is the Drell-Yan production of electrons or muons ($q\bar{q} \rightarrow Z/\gamma^* \rightarrow \ell^+\ell^-$, where $\ell = e, \mu$) with spurious \cancel{E}_T . Both of the above background contributions are estimated using data-based methods [10]. The remaining background contributions are from the Drell-Yan production of τ leptons and diboson (WW, WZ, ZZ) production which are estimated using Monte-Carlo (MC) simulation. The detailed description of the background estimation can be found in [10]. The numbers of expected and observed events passing dilepton selection are given in Table I. Statistical and systematic uncertainties are combined for the numbers of events. The correlations among signal and backgrounds systematic uncertainties are considered for the total numbers of events. There is a good agreement between data and expectations from $t\bar{t}$ production and background contributions (this holds also for “ b -tag” and “non-tag” subsamples individually).

We use the $\cos\theta^*$ of the leptons defined above to determine the W -boson polarization fractions. In order to reconstruct $\cos\theta^*$, the full event kinematics of $t\bar{t}$ decay chain must be reconstructed. The dilepton channel presents an under-constrained system due to the two un-

TABLE I: Expected and observed numbers of signal and background events after the dilepton selection assuming $\sigma_{t\bar{t}} = 6.7$ pb ($m_{top} = 175$ GeV/ c^2).

Source	Events		
Diboson	17.5	\pm	4.6
$Z/\gamma^* \rightarrow \tau\tau$	12.3	\pm	2.2
$Z/\gamma^* \rightarrow ee + \mu\mu$	22.4	\pm	3.2
Fakes	53.7	\pm	14.7
Total background	105.8	\pm	17.2
$t\bar{t}$ ($\sigma = 6.7$ pb)	222.4	\pm	10.6
Total SM expectation	328.2	\pm	27.6
Observed	343		

detected neutrinos. We use a simple modification of the kinematic method previously developed for the measurement of the top-quark mass, denoted as the KIN method in [17]. We solve the kinematic equations by Newton’s method for nonlinear systems of equations using the top-quark mass constraint with $m_{top} = 175$ GeV/ c^2 . In principle each event provides two measurements of $\cos\theta^*$. However, some events do not have kinematic solutions under our assumptions, and these events are discarded.

In order to perform a fit to the $\cos\theta^*$ distribution we create templates using $t\bar{t}$ MC simulated samples for exclusive left-handed, longitudinal and right-handed W -bosons using a customized HERWIG [18, 19] MC generator. We create the templates separately for “ b -tag” and “non-tag” subsamples which turn out to be similar. Figure 1 shows the templates for the inclusive sample for both the signal and background.

Due to various selection and reconstruction effects (e.g., we consider the two highest E_T jets as jets coming from b -quark hadronization while there is a possibility that one of these two jets comes from initial (ISR) or final (FSR) state gluon radiation) the templates vary significantly from the theoretical distributions in Eq. (1). The effect of the lepton E_T and the isolation cut is seen as a softening of the theoretical peaks near $\cos\theta^* = -1$. Furthermore, the KIN reconstruction method requires the lepton-jet- \cancel{E}_T mass to be close to the mass of the top quark so that the reconstruction is inefficient for high lepton-jet pair masses ($\cos\theta^* \simeq +1$). This gives a polarization-dependent reconstruction efficiency of about 95%, 92%, and 87%, respectively, for left-handed, longitudinal, and right-handed W -bosons. For the background events, the reconstruction efficiency is only 71%. There are also differences in the acceptance of dilepton events. The difference can be as large as about 30%, as observed between events with two left-handed W bosons and those with two longitudinal W bosons, where the latter has a relatively larger acceptance than the former. This is mainly due to the dependence of the acceptance on the lepton p_T and isolation (leptons from left-handed

W -bosons tend to be less isolated and have smaller p_T).

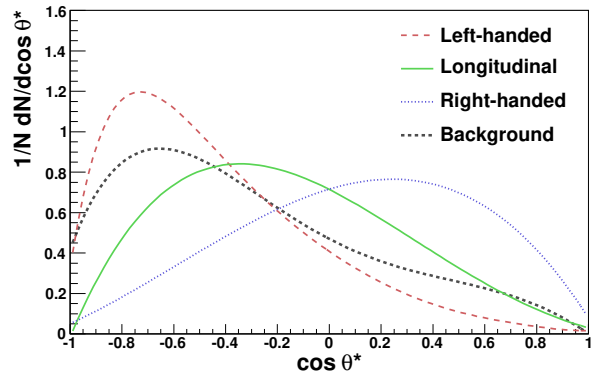


FIG. 1: The signal templates for left-handed, longitudinal and right-handed W -bosons together with the background template for the inclusive dilepton selection.

We combine the signal and background templates taking into account the above W polarization dependent efficiencies. We use an unbinned likelihood method which determines the f_0 and f_+ polarization fractions that best correspond to the observed $\cos\theta^*$ distribution. A Gaussian constraint on the number of background events and a Poisson constraint on the total number of observed events in data are included in the likelihood formula. We multiply the likelihoods for “ b -tag” and “non-tag” subsamples to arrive at the final likelihood. The method has been extensively tested in simulated samples across the full range of physically possible values of f_0 and f_+ parameters. From these tests, we obtain small corrections to the measured values of f_0 and f_+ .

The determination of W -boson polarization fractions by our method is sensitive to different sources of theoretical and experimental uncertainties, such as the MC simulated templates, the jet reconstruction algorithms, and jet corrections. We have generated ensembles of simulated experiments in order to estimate these systematic uncertainties. One of the largest sources of systematic uncertainty comes from the jet energy scale (JES). We have studied this uncertainty by changing the corrections by $\pm 1\sigma$ of the JES uncertainty [15]. Another large systematic uncertainty is modeling of the signal which we estimate as variations in the ISR and FSR, using different parton distribution functions (PDF) and different MC generators (see [10] for details). We estimate the systematic uncertainty due to the background template shape by changing each individual background within its rate uncertainty thus changing the overall shape. We then combine all these shifts (in quadrature) to obtain an overall background shape uncertainty. The uncertainty in the total number of expected background events is taken into account in the fitting procedure where the amount of background is allowed to float. The method-specific

systematic uncertainties are due to limited statistics of the signal and background templates and are evaluated by fluctuating the templates bin-by-bin. An additional (small) uncertainty is due to the instantaneous luminosity which determines the mean number of interactions per bunch crossing. The systematic uncertainties are summarized in Table II, with the total systematic uncertainty of the measurement being the sum in quadrature of all the partial systematic uncertainties from the various sources.

TABLE II: Summary of systematic uncertainties.

Source	Δf_0^{1D}	Δf_+^{1D}	Δf_0^{2D}	Δf_+^{2D}
Jet energy scale	0.033	0.019	0.002	0.020
Generators	0.035	0.019	0.016	0.011
ISR/FSR	0.024	0.010	0.040	0.017
PDF	0.010	0.003	0.025	0.009
Background shape	0.012	0.005	0.023	0.010
Template statistics				
Signal	0.010	0.005	0.024	0.012
Background	0.007	0.004	0.015	0.007
Instant. luminosity	0.016	0.008	0.013	0.002
Total	0.059	0.031	0.063	0.034

We assume a fixed top-quark mass of $m_{top} = 175$ GeV/ c^2 in our dilepton measurement. However, as already noted, within the SM the fraction of W -bosons with a given polarization directly depends on the top-quark and W -boson masses. We do not include this effect in the systematic uncertainties for the result in the dilepton channel. Rather, we provide the m_{top} -dependence of the reconstructed fractions. We estimate that there is a linear shift in reconstructed f_0 of $\pm(0.004 \pm 0.007)$ and $\pm(0.012 \pm 0.004)$ and in reconstructed f_+ of $\pm(0.005 \pm 0.004)$ and $\pm(0.006 \pm 0.002)$ per ± 1 GeV/ c^2 change in the top-quark mass for 2D and 1D measurements, respectively. In order to be close to the world average top-quark mass [5], we use the top-quark mass dependence (presented above) to correct the result to a top-quark mass of 172.5 GeV/ c^2 .

There are 304 events (118 in “ b -tag” and 186 in “non-tag” subsamples) passing dilepton selection and kinematic reconstruction, consistent with the SM expectation of 284.3 ± 22.7 events. The comparison of $\cos \theta^*$ distribution between data and the expectations for SM $t\bar{t}$ signal and background can be seen in Fig. 2. There is a good agreement between data and the SM expectation ($\chi^2 = 6.5$ for 9 degrees of freedom, corresponding to a p -value of 69%).

We perform a model-independent simultaneous determination of both f_0 and f_+ fractions: $f_0 = 0.70^{+0.18}_{-0.17}$ (stat) and $f_+ = -0.09 \pm 0.09$ (stat). There is a strong negative correlation of -0.88 between the statistical uncertainties of f_0 and f_+ . We also measure each polarization fraction when the other is fixed to its SM

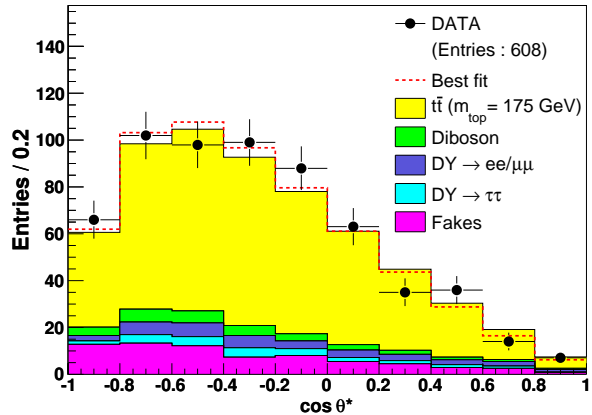


FIG. 2: The $\cos \theta^*$ distributions for data, the expected SM $t\bar{t}$ signal and background, and the best fit value. Each event has two entries in the histogram.

value. We measure $f_0 = 0.56 \pm 0.09$ (stat) when f_+ is so fixed and measure $f_+ = -0.09 \pm 0.04$ (stat) when f_0 is so fixed. We also find $f_+ < 0.07$ at 95% C.L. when f_0 is so fixed following a Bayesian procedure assuming a constant a priori probability for f_+ across the physically possible range.

The CDF measurement performed in the single-lepton channel obtained the following result [6], assuming a top-quark mass of 172.5 GeV/ c^2 : $f_0 = 0.90 \pm 0.11$ (stat) ± 0.06 (syst) and $f_+ = -0.19 \pm 0.07$ (stat) ± 0.06 (syst) with the correlation of -0.59 between f_0 and f_+ . This is consistent with the result presented in this Letter. We combine both results using the analytic best linear unbiased estimator method [20, 21]. We include the systematic uncertainties corresponding to a ± 1.1 GeV/ c^2 uncertainty on m_{top} [5]. The results of the dilepton and single-lepton channels are statistically independent. There is a strong negative correlation of the statistical uncertainty between the f_0 and f_+ observables for both channels as mentioned above. The systematic uncertainties are theoretically dominated and are assumed to be 100% correlated between the measurements, with the exception of the method-specific systematic uncertainties (signal and background template statistics) which are treated as uncorrelated. The luminosity-related systematic uncertainty applies only to the dilepton measurement. For a given measurement, we assume that the f_0 and f_+ uncertainties are 100% anti-correlated for each systematic uncertainty category. Table III presents the full correlation matrix between the measurements and their weights in the combination. The combined result for the simultaneous measurement is $f_0 = 0.84 \pm 0.09$ (stat) ± 0.05 (syst) and $f_+ = -0.16 \pm 0.05$ (stat) ± 0.04 (syst). The combination has a χ^2 value of 0.99 for two degrees of freedom, corresponding to a p -value of 61% for consistency be-

TABLE III: The correlation coefficients among the measurements and their weights in the f_0 and f_+ combined result. The results from single-lepton channel are labeled as ‘LJ’, the dilepton results as ‘DIL’.

Measurement	Correlation matrix				Weight for f_0 (%)	Weight for f_+ (%)
	LJ f_0	DIL f_0	LJ f_+	DIL f_+		
LJ f_0	1				80.6	-21.8
DIL f_0	0.13	1			19.4	21.8
LJ f_+	-0.72	-0.15	1		18.9	24.0
DIL f_+	-0.12	-0.88	0.16	1	-18.9	76.0

tween the input measurements. The combined values of f_0 and f_+ have a correlation coefficient -0.81 . We also combine the measurements of one polarization fraction when the other one is fixed to its SM expected value. In this case, we arrive at $f_0 = 0.64 \pm 0.06(\text{stat}) \pm 0.05(\text{syst})$ (f_+ is fixed) and $f_+ = -0.07 \pm 0.02(\text{stat}) \pm 0.04(\text{syst})$ (f_0 is fixed). The combination for f_0 (f_+) has a χ^2 of 1.04 (0.61) for one degree of freedom, corresponding to a p-value of 31% (44%) for consistency between the input measurements.

To summarize, we have performed a measurement of W -boson polarization fractions in top-quark dilepton decays. Our method is the first model-independent measurement of the W polarization in the dilepton channel from CDF. We have also combined our dilepton measurement with our previous measurement in the single-lepton channel. Our results are consistent with the SM expectations and do not require the introduction of new physics. They agree with the results obtained by the D0 and ATLAS collaborations [7, 8] which are of comparable precision.

We thank the Fermilab staff and the technical staffs of the participating institutions for their vital contributions. This work was supported by the U.S. Department of Energy and National Science Foundation; the Italian Istituto Nazionale di Fisica Nucleare; the Ministry of Education, Culture, Sports, Science and Technology of Japan; the Natural Sciences and Engineering Research Council of Canada; the National Science Council of the Republic of China; the Swiss National Science Foundation; the A.P. Sloan Foundation; the Bundesministerium für Bildung und Forschung, Germany; the Korean World Class University Program, the National Research Foundation of Korea; the Science and Technology Facilities Council and the Royal Society, UK; the Institut National de Physique Nucleaire et Physique des Partic-

ules/CNRS; the Russian Foundation for Basic Research; the Ministerio de Ciencia e Innovación, and Programa Consolider-Ingenio 2010, Spain; the Slovak R&D Agency; the Academy of Finland; and the Australian Research Council (ARC).

- [1] T. Aaltonen *et al.* (CDF Collaboration), Phys. Rev. Lett. **105**, 232003 (2010).
- [2] V. M. Abazov *et al.* (D0 Collaboration), Phys. Rev. Lett. **106**, 022001 (2011).
- [3] J. A. Aguilar-Saavedra *et al.*, Eur. Phys. J. C **50**, 519 (2007).
- [4] K. Nakamura *et al.* (Particle Data Group), J. Phys. G **37**, 075021 (2010) and 2011 partial update for the 2012 edition.
- [5] T. Aaltonen *et al.* (CDF and D0 Collaborations), arXiv:1007.3178 [hep-ex].
- [6] T. Aaltonen *et al.* (CDF Collaboration), Phys. Rev. Lett. **105**, 042002 (2010).
- [7] V. M. Abazov *et al.* (D0 Collaboration), Phys. Rev. D **83**, 032009 (2011).
- [8] G. Aad *et al.* (ATLAS Collaboration), JHEP06, 088 (2012).
- [9] D. Acosta *et al.* (CDF Collaboration), Phys. Rev. D **71**, 032001 (2005).
- [10] T. Aaltonen *et al.* (CDF Collaboration), Phys. Rev. D **82**, 052002 (2010).
- [11] CDF uses a cylindrical coordinate system with the z axis along the proton beam axis. Pseudorapidity is $\eta \equiv -\ln \tan(\theta/2)$, where θ is the polar angle relative to the proton beam direction and ϕ is the azimuthal angle while $p_T = |p| \sin \theta$, $E_T = E \sin \theta$.
- [12] For the muons, transverse momentum p_T rather than transverse energy E_T is considered in the text.
- [13] The missing transverse energy (\vec{E}_T) is defined by $\vec{E}_T = -\sum_i E_T^i \hat{n}_i$, where i denotes calorimeter tower number with $|\eta| < 2.5$, and \hat{n}_i is a unit vector perpendicular to the beam axis and pointing at the i^{th} calorimeter tower. We also define $E_T = |\vec{E}_T|$.
- [14] A jet is defined as a fixed-cone cluster in the calorimeter with a cone size of 0.4 in azimuth-pseudorapidity (η) space.
- [15] A. Bhatti *et al.* (CDF Collaboration), Nucl. Instrum. Methods A **566**, 375 (2006).
- [16] D. Acosta *et al.* (CDF Collaboration), Phys. Rev. D **71**, 052003 (2005).
- [17] A. Abulencia *et al.* (CDF Collaboration), Phys. Rev. D **73**, 112006 (2006).
- [18] E. H. Guillian, Ph.D. thesis, University of Michigan, 1999, Fermilab-Thesis-1999-51.
- [19] G. Corcella *et al.*, J. High Energy Phys. 01 (2001) 10.
- [20] L. Lyons, D. Gibaut, and P. Clifford, Nucl. Instrum. Methods A **270** (1988) 110.
- [21] A. Valassi, Nucl. Instrum. Methods A **500** (2003) 391.